Current Biology, Vol. 13, 329–332, February 18, 2003, ©2003 Elsevier Science Ltd. All rights reserved. PII S0960-9822(03)00051-4

The Force-Velocity Relationship for the Actin-Based Motility of *Listeria monocytogenes*

James L. McGrath,[1,4,5] Narat J. Eungdamrong,[2,4] Charles I. Fisher,[1] Fay Peng,[1] Lakshminarayanan Mahadevan,[3,6] Timothy J. Mitchison,[2] and Scot C. Kuo[1,*]
[1]Department of Biomedical Engineering
Johns Hopkins University
720 Rutland Avenue
Ross 724
Baltimore, Maryland 21205
[2]Department of Cell Biology
Harvard Medical School
250 Longwood Avenue
Boston, Massachusetts 02115
[3]Department of Mechanical Engineering
Massachusetts Institute of Technology
77 Massachusetts Avenue
Cambridge, Massachusetts 02139

Summary

The intracellular movement of the bacterial pathogen *Listeria monocytogenes* has helped identify key molecular constituents of actin-based motility (recent reviews [1–4]). However, biophysical as well as biochemical data are required to understand how these molecules generate the forces that extrude eukaryotic membranes. For molecular motors and for muscle, force-velocity curves have provided key biophysical data to distinguish between mechanistic theories. Here we manipulate and measure the viscoelastic properties of tissue extracts to provide the first force-velocity curve for *Listeria monocytogenes.* We find that the force-velocity relationship is highly curved, almost biphasic, suggesting a high cooperativity between biochemical catalysis and force generation. Using high-resolution motion tracking in low-noise extracts, we find long trajectories composed exclusively of molecular-sized steps. Robust statistics from these trajectories show a correlation between the duration of steps and macroscopic *Listeria* speed, but not between average step size and speed. Collectively, our data indicate how the molecular properties of the *Listeria* polymerization engine regulate speed, and that regulation occurs during molecular-scale pauses.

Results and Discussion

To mechanically slow the actin-based motility of *Listeria* in bovine brain extracts, we used methylcellulose as a viscoelastic thickening agent. Unlike ideal viscous solutions that would slow all biochemical rates [5], the large molecules of methylcellulose do not perturb the kinetics of actin assembly, particularly ARP2/3-dependent assembly in extracts (Figure 1A). To facilitate mixing of methylcellulose with motility solutions and *Listeria*, we exploited the temperature-dependent solubility of methylcellulose powder to dissolve it in situ within each microscope slide (see Supplementary Material available with this article online). However, microheterogeneities and wall effects from thin microscope chambers ($\sim$12 μm) preclude calculating mechanical drag forces from bulk rheological measurements of methylcellulose. To locally measure viscoelastic moduli ($|G^*(\omega)|$), we used laser-tracking microrheology (LTM; [6, 7]) to track the Brownian motion of three or more surface-modified polystyrene particles immediately near motile bacteria (Figure 2B). To prevent spurious local mechanics, blocking chemistries are required to suppress nonspecific actin polymerization on bare tracer particles. Using the generalized Stokes equation $F_{drag} = 6\pi SaV\eta(\dot{\gamma})$ to calculate drag forces on bacteria, we account for the size (minor radius a), shape (S), speed (V), and the steady-shear viscosity $\eta(\dot{\gamma})$ at a shear rate of $\dot{\gamma} = V/2a$. For general non-Newtonian fluids, dynamic viscosity $\eta^*(\omega)$, measured from oscillatory deformations at frequency ω, cannot predict the steady-shear viscosity $\eta(\dot{\gamma})$ experienced by steadily moving *Listeria*. However, methylcellulose solutions obey the Cox-Merz rule, which states that the steady-shear viscosity $\eta(\dot{\gamma})$ is empirically the same as the dynamic viscosity $|\eta^*(\omega)|$ when $\dot{\gamma} = \omega$ [8]. With the simple identity, $\eta^*(\omega) = G^*(\omega)/i\omega$, we can use this approach to calculate drag forces from LTM measurements (see Supplementary Materials).

Across 45 bacteria, we find a highly curvilinear relationship between *Listeria* speeds and the drag forces due to local viscoelastic moduli (Figure 3). Although the moduli of extracts spans $\sim$500-fold range, *Listeria* were only slowed by a factor of $\sim$20. Despite our best efforts, we could not fully stall *Listeria* and can only put a lower bound of 200 pN for stalling forces. As shown in the inset of Figure 3, mechanical power increases as load increases. To determine the molecular basis of this self-strengthening behavior, we used fluorescence microscopy to quantify the amount of actin in these tails. A 1.6-fold increase in average density of actin-specific fluorescence corresponds to a $\sim$3-fold increase in mechanical power and a $\sim$20-fold increase in forces (see Supplementary Materials). These data indicate cooperative phenomena because larger forces can be generated by a small amount of additional actin polymerization.

As in living host cells [9], *Listeria* in brain extracts frequently moved with monomer-spaced pauses (Figure 1B). For tails that are not anchored, we note that actin monomer insertion should move the tail and bacterium in opposite directions, thus necessarily reducing the apparent size of bacterial displacements. High concentrations of methylcellulose ($>$1%) were required to suppress large-scale Brownian motions of bacteria and their tails. Quantifying the moduli of these thick solutions are

*Correspondence: skuo@bme.jhu.edu
[4]These authors contributed equally to this work.
[5]Present address: Biomedical Engineering Department, University of Rochester Medical Center, 601 Elmwood Avenue, Box 639, Rochester, New York 14642.
[6]Present address: Applied Mathematics and Theoretical Physics, Cambridge University, Cambridge, CB3 9EW, United Kingdom.

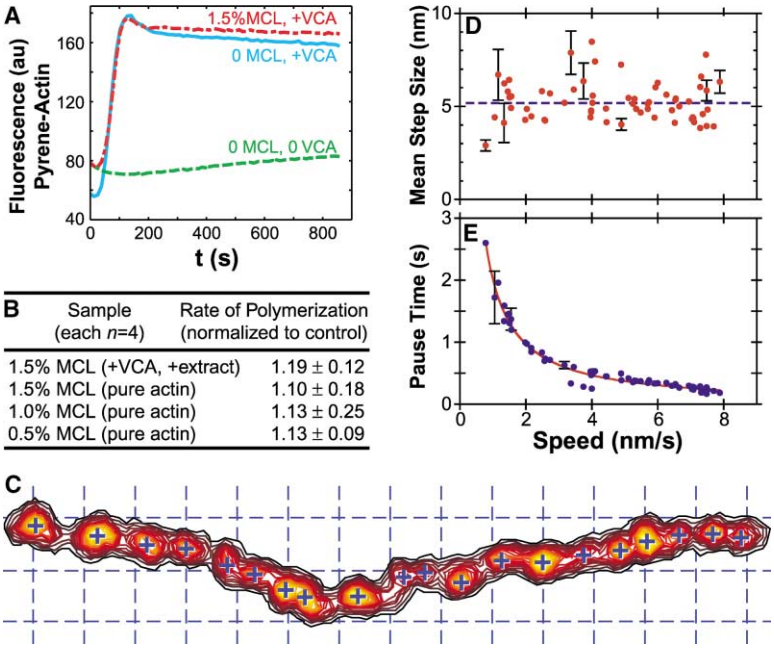

Figure 1. Methylcellulose Does Not Slow Actin Polymerization and *Listeria* Speeds Correlate with Pause Duration, Not Step Distance

(A) Methylcellulose does not slow stimulated actin polymerization in extracts. Curves show kinetics of pyrene-actin polymerization stimulated by the ARP2/3 interacting domain of N-WASP (VCA peptide) in extracts containing 0% methylcellulose (blue) and 1.5% methylcellulose (red). Recombinant GST-VCA was purified as described previously [27] and used at 50 nM. Also shown is the unstimulated polymerization of actin (no VCA added) in extract (green).

(B) Methylcellulose does not slow the polymerization rate of pure actin. The table compares the initial rate of polymerization normalized to controls containing no methylcellulose.

(C) Thick methylcellulose reveals step-like motion in extracts. For methylcellulose concentrations <1%, extraneous motions, such as pivoting tails, are large enough to obscure steps. The data shown are for 1.5% methylcellulose and grid lines are spaced 5.4 nm. Positional histograms are generated from *Listeria* trajectories as previously described [9], and blue crosses represent pause events detected by automated detection software (see Supplementary Materials). In our current equipment, mechanical resonances obscure the Brownian motion of particles in the thick methylcellulose solutions needed to reveal steps. Thus, it is not possible to measure the viscoelasticity of these solutions using microrheology.

(D) The average size of steps is independent of average *Listeria* velocity. The average step size over 66 trajectories (13 different bacteria; 1152 steps) is 5.2 ± 0.15 nm. Representative error bars show standard error of the mean for step sizes within that trajectory.

(E) The duration of pauses correlates inversely with average *Listeria* velocity. Average velocity and the mean pause time are calculated for each of 66 trajectories.

beyond the capabilities of our current LTM equipment, and so our force-velocity analysis does not extend to the regime required for observing molecular-scale pausing. Analyzing 66 trajectories (containing 1152 steps), the distance between pauses is 5.2 ± 0.15 nm. As shown in Figure 1C, the average step size during a trajectory does not correlate with the average speed during that trajectory, suggesting that the stepping phenomenon is an invariant feature of *Listeria* motility. The average duration of pauses, however, shows a strong inverse correlation with *Listeria* speeds (Figure 1D). We conclude that the regulation of *Listeria* speed occurs through changes in the duration of these molecular-sized pauses, at least under the conditions required to observe steps.

Explanations for monomer-sized steps fall into three categories depending on the number of actin filaments that limit motion. Stretched by the pressure generated by other actin filaments, a single tethering filament might provide a transient template for limiting the motions of the bacterium [9]. Rebinding to adjacent actin monomers along the sides of this filament would generate monomer-sized displacements. Incorporating putative nucleotide-dependent binding between *Listeria* and F-actin, recent calculations develop more fully the stochastic generation of such filament templates (actoclampin, [10]). Such single-filament explanations are only plausible for forces less than the breaking point of an individual actin filament (~600 pN; [11]). Alternatively, when several (~5) tethered filaments are limiting, dissociation of one of the limiting filaments causes the other limiting filaments to "stretch" [12]. Molecular-sized steps result from the combination of filament compliances of appropriate magnitudes. At the other extreme, many filaments restrain bacteria and all tethering must release cooperatively to produce steps. Mechanical cooperativity could occur when propulsive stresses within the tail network exceed a threshold for frictional resistance, as suggested for mesoscopic, micrometer-sized stepping phenomena [13, 14]. However, the notion of friction is fundamentally a mesoscopic generalization [15] and must be recast as molecular interactions to explain molecule-sized steps.

More constraining than molecule-sized steps, the unusually curved force-velocity relationship for *Listeria* demands newer biophysical theories for its actin-based motility. Until recently, theoretical models predicted gentle exponential-like force-velocity relationships that cannot be parametrically altered to fit the sharply curved relationship that we have measured. Despite ambiguities in estimating the number of actin filaments in tails, these models predict numerical values that can differ from our measurements by orders of magnitude. In a mesoscopic gel model, Gerbal and colleagues suggest that, like an inflating balloon, stretching stresses within the tail increase as the crosslinked actin gel expands radially from the curved bacterial surface [13]. They predicted a force-velocity relationship that is gently curved and cannot fit our data. Furthermore, this model predicts that *Listeria* will only slow when forces are strong enough to deform crosslinked gels (0.1–1 nN). Instead, our data show velocities sensitive to loads ~10 pN, a level adequate to bend single actin filaments [16] rather than the gel. In the Brownian ratchet models, positional

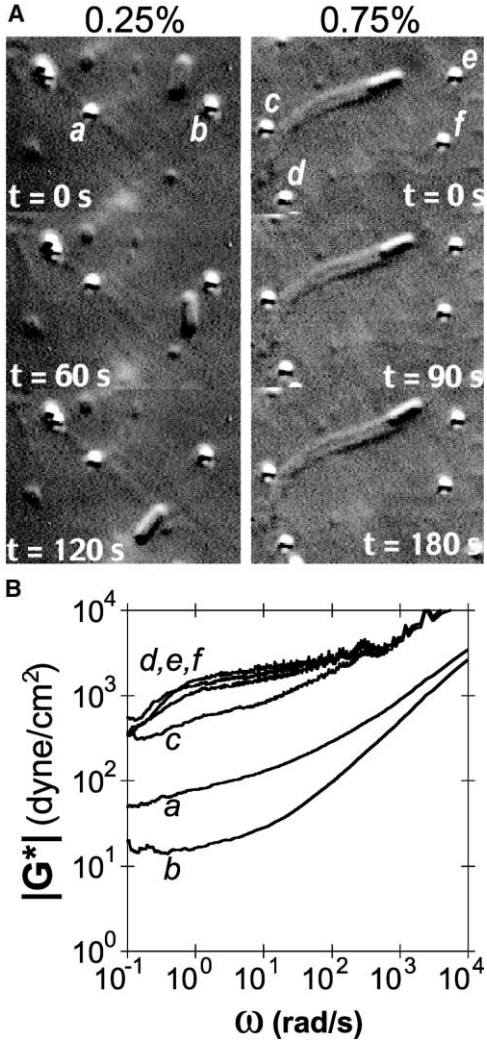

Figure 2. Microrheology Experiments

(A) *Listeria* move slower and tails emerge in extracts thickened with methylcellulose. *Listeria* are moving at ~3 μm/min in the left column (0.25% methylcellulose) and ~0.4 μm/min in the right column (0.75% methylcellulose).

(B) Viscoelastic spectra for the particles shown in (A). Dynamic moduli, $|G^*(\omega)|$, as a function of oscillatory frequency, ω, were measured using LTM. Particles *a* and *b* around the fast moving *Listeria* reveal an environment an order of magnitude weaker than the environment around the slow moving *Listeria* (particles *c*, *d*, *e*, and *f*) at the frequencies most relevant to *Listeria* motility ($\omega < 1$ rad/s). For these two bacteria, the drag forces and their velocities are 8.4 pN at 45 nm/s and 80 pN at 7.3 nm/s for 0.25% and 0.75% methylcellulose, respectively.

fluctuations either of bacteria or of the ends of actin filaments allow room for monomer intercalation to generate forces [16, 17]. These versions of the Brownian ratchet model predict exponential force-velocity relationships with gentle curvature. In a "clamped filament" model, a putative actin clamp mechanism latches onto subunits carrying ATP and then releases after hydrolysis to allow the axial diffusion of filaments [10]. The clamped filament model predicts a broad range of forces where velocity is relatively constant, and this range extends ~6 pN/filament (~500 pN for 80 filaments).

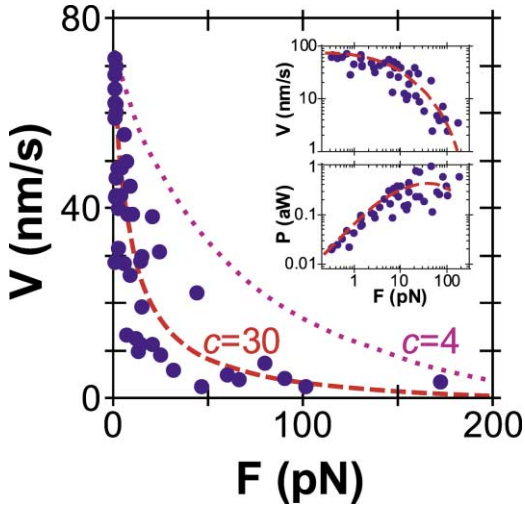

Figure 3. Force and Power Generated by *Listeria*

Bacterial velocities decrease with increasing drag forces. Varying methylcellulose concentrations between 0.25% and 1% caused *Listeria* to slow over 20-fold. Using probe particles adjacent to motile *Listeria*, viscoelastic spectra were measured to calculate drag forces (see Supplementary Materials). Inset top: The same data was plotted on logarithmic axes. Inset bottom: Mechanical power increases with drag forces. Mechanical power in attowatts was calculated as the product of velocity and force. The smooth curves derive from a phenomenological least-squares curve-fitting to the normalized Hill model for muscle [18]: $F/F_{max} = (1 - v/v_{max})/(1 + cv/v_{max})$ with $F_{max} = 250 \pm 120$ pN, $v_{max} = 74 \pm 50$ nm/s, and $c = 31 \pm 44$. Calculated with the same F_{max} and v_{max}, the inset shows for comparison a curve with $c = 4$ that is typical of muscle.

To gain insight into mechanisms producing curvature in force-velocity curves, we note that the force-velocity relationship of *Listeria* resembles the hyperbolic relationship of muscle, but with much higher curvature (parametric curvature factors: $c = \sim 30$ for *Listeria*, inset Figure 3; $c = 1.3$–6 for muscle [18–20]). Akin to myosin in muscle, bacterially bound ActA, and host cell ARP2/3, G-actin and F-actin form a transient complex [1] that both propels and restricts *Listeria* motion. Propulsion occurs because the quaternary complex efficiently nucleates new actin filament branches, but ARP2/3 remains at the nodes of branches [21] and does not slide along the "mother" filament [22]. If long-lived, association of bacterially bound ActA to these nodal ARP2/3 necessarily "drags" on the work of the tail by acting as an internal load. Other proteins, such as F-actin binding by VASP bound to ActA [23], may contribute to the internal loading. The intrinsic lifetime of the tail bound molecular complexes therefore defines a natural velocity threshold of behavior. At faster velocities, bacterial tail binding complexes are long lived enough to become internally stretched and reduce the net forces generated. Internal strain may accelerate the disassembly of these complexes. At slower velocities, bacterial tail binding complexes naturally disassemble without internal strain, and the actin density of the tail should be maximal because there is more time to nucleate filaments. Our fluorescence data document such an increase in actin density at slower velocities (see Supplementary Materials). Like muscle models [24], we expect

that longer-lived tail associations will increase the curvature of the force-velocity relationship of *Listeria* models. The importance of tail associations has been very recently incorporated in the elastic Brownian ratchet model to produce a "tethered" ratchet model [12]. The model predicts a sharply curved force-velocity relationship that is quantitatively similar to our data.

The biochemical complexity of *Listeria*'s actin-based motility [25] ensures that the absolute values of the force-velocity relationship reported here are not universal. Nonetheless, the unusually sharp curvature of the force-velocity relationship reveals the underlying antagonistic mechanics. Tail binding accelerates propulsion biochemically but restrains mechanically. Combined with strain-dependent release, the sharp curvature suggests very long-lived tail binding complexes in *Listeria*. Although ARP2/3 demonstrates both antagonistic functions, VASP is another possible candidate. VASP probably links bacteria to the barbed ends of actin [26], while accelerating motility [25]. Because the duration of monomer-spaced pauses correlates strongly with velocity, unbinding the tail appears to be molecularly rate-limiting for *Listeria* motility. Monomer-spaced pauses and the sharply curved force-velocity relationship may be facets of the same molecular tail binding events.

Supplementary Material

Additional methodological detail and two supplementary figures showing that actin tail densities of *Listeria* increase with higher loads and that velocities decrease with effective viscosity are available at http://images.cellpress.com/supmat/supmatin.htm.

Acknowledgments

We thank James Harden, Anthony Beris, and Colin Keary for insightful discussions on drag forces in viscoelastic fluids. We thank Eric Osborn and John Hartwig for material and help with actin polymerization assays. N.J.E., T.J.M., and L.M. were supported by grants from the Center for Biomedical Engineering at M.I.T. and the Edgerly Foundation. J.L.M. and S.C.K. were supported by grants from the National Science Foundation and the Whitaker Foundation. S.C.K. and T.J.M. are supported by grants from the National Institutes of Health.

Received: November 13, 2002
Revised: December 9, 2002
Accepted: December 10, 2002
Published: February 18, 2003

References

1. Higgs, H.N., and Pollard, T.D. (2001). Regulation of actin filament network formation through ARP2/3 complex: activation by a diverse array of proteins. Annu. Rev. Biochem. *70*, 649–676.
2. Pantaloni, D., Le Clainche, C., and Carlier, M.-F. (2001). Mechanism of actin-based motility. Science *292*, 1502–1506.
3. Bear, J.E., Krause, M., and Gertler, F.B. (2001). Regulating cellular actin assembly. Curr. Opin. Cell Biol. *13*, 158–166.
4. Cameron, L.A., Giardini, P.A., Soo, F.S., and Theriot, J.A. (2000). Secrets of actin-based motility revealed by a bacterial pathogen. Nat. Rev. Mol. Cell Biol. *1*, 110–119.
5. Hunt, A., Gittes, F., and Howard, J. (1994). The force exerted by a single kinesin molecule against a viscous load. Biophys. J. *67*, 766–781.
6. Mason, T.G., Ganesan, K., Van Zanten, J.H., Wirtz, D., and Kuo, S.C. (1997). Particle tracking microrheology of complex fluids. Phys. Rev. Lett. *79*, 3282–3285.
7. Yamada, S., Wirtz, D., and Kuo, S.C. (2000). Mechanics of living cells measured by laser tracking microrheology. Biophys. J. *78*, 1736–1747.
8. Haque, A., and Morris, E.R. (1993). Thermogelation of methylcellulose. Part I: molecular structures and processes. Carbohydr. Polym. *22*, 161–173.
9. Kuo, S.C., and McGrath, J.L. (2000). Steps and fluctuations of *Listeria monocytogenes* during actin-based motility. Nature *407*, 1026–1029.
10. Dickinson, R.B., and Purich, D.L. (2002). Clamped-filament elongation model for actin-based motors. Biophys. J. *82*, 605–617.
11. Tsuda, Y., Yasutake, H., Ishijima, A., and Yanagida, T. (1996). Torsional rigidity of single actin filaments and actin-actin bond breaking force under torsion measured directly by in vitro micromanipulation. Proc. Natl. Acad. Sci. USA *93*, 12937–12942.
12. Mogilner, A., and Oster, G. (2003). Force generation by actin polymerization II: the elastic ratchet and tethered filaments. Biophys. J., in press.
13. Gerbal, F., Chaikin, P., Rabin, Y., and Prost, J. (2000). An elastic analysis of *Listeria monocytogenes* propulsion. Biophys. J. *79*, 2259–2275.
14. Bernheim-Groswasser, A.B., Wiesner, S., Golsteyn, R.M., Carlier, M.F., and Sykes, C. (2002). The dynamics of actin-based motility depend on surface parameters. Nature *417*, 308–311.
15. Howard, J. (2001). Mechanics of Motor Protins and the Cytoskeleton (Sunderland, MA: Sinauer Associates).
16. Mogilner, A., and Oster, G. (1996). Cell motility driven by actin polymerization. Biophys. J. *71*, 3030–3045.
17. Peskin, C.S., Odell, G.M., and Oster, G.F. (1993). Cellular motions and thermal fluctuations: the Brownian ratchet. Biophys. J. *65*, 316–324.
18. Fung, Y.C. (1993). Biomechanics: Mechanical Properties of Living Tissues, second edition (New York, NY: Springer-Verlag).
19. Chiu, Y.C., Ballou, E.W., and Ford, L.E. (1987). Force, velocity, and power changes during normal and potentiated contractions of cat papillary muscle. Circ. Res. *60*, 446–458.
20. Brutsaert, D.L., and Sonnenblick, E.H. (1969). Force-velocity-length-time relations of the contractile elements in heart muscle of the cat. Circ. Res. *24*, 137–149.
21. Cameron, L.A., Svitkina, T.M., Vignjevic, D., Theriot, J.A., and Borisy, G.G. (2001). Dendritic organization of actin comet tails. Curr. Biol. *11*, 130–135.
22. Volkmann, N., Amann, K.J., Stoilova-McPhie, S., Egile, C., Winter, D.C., Hazelwood, L., Heuser, J.E., Li, R., Pollard, T.D., and Hanein, D. (2001). Structure of Arp2/3 complex in its activated state and in actin filament branch junctions. Science *293*, 2456–2459.
23. Laurent, V., Loisel, T.P., Harbeck, B., Wehman, A., Grobe, L., Jockusch, B.M., Wehland, J., Gertler, F.B., and Carlier, M.F. (1999). Role of proteins of the Ena/VASP family in actin-based motility of *Listeria monocytogenes*. J. Cell Biol. *144*, 1245–1258.
24. Huxley, A.F. (1957). Muscle structure and theories of contraction. Prog. Biophys. Biophys. Chem. *7*, 255–318.
25. Loisel, T.P., Boujemaa, R., Pantaloni, D., and Carlier, M.-F. (1999). Reconstitution of actin-based motility of *Listeria* and *Shigella* using pure proteins. Nature *401*, 613–615.
26. Bear, J.E., Svitkina, T.M., Krause, M., Schafer, D.A., Loureiro, J.J., Strasser, G.A., Maly, I.V., Chaga, O.Y., Cooper, J.A., Borisy, G.G., et al. (2002). Antagonism between Ena/VASP proteins and actin filament capping regulates fibroblast motility. Cell *109*, 509–521.
27. Rohatgi, R., Ma, L., Miki, H., Lopez, M., Kirchhausen, T., Takenawa, T., and Kirschner, M.W. (1999). The interaction between N-WASP and the Arp2/3 complex links Cdc42-dependent signals to actin assembly. Cell *97*, 221–231.